Nonaxisymmetric flow in a finite-length cylinder with a rotating magnetic field

L. Martin Witkowski and J. S. Walker
Department of Mechanical and Industrial Engineering, University of Illinois, Urbana, Illinois 61801

P. Marty
Laboratoire des Ecoulements Geophysiques et Industriels, B. P. 53, 38041, Grenoble, France

(Received 30 October 1998; accepted 23 March 1999)

This paper treats the flow of an electrically conducting liquid in an insulating cylinder with a spatially uniform, transverse, rotating magnetic field. The frequency of the externally applied magnetic field is sufficiently low that this field penetrates throughout the liquid. Previous researchers have treated the steady, axisymmetric flow driven by the azimuthal average of the electromagnetic body force. This paper presents an analytical solution for the nonaxisymmetric flow perturbation driven by the deviation of the body force from its azimuthal average. For the magnetic field strengths and frequencies currently used in crystal-growth processes, the values of the interaction parameter N and the Reynolds number Re, both based on the frequency of the magnetic field, are small and large, respectively. The results of the appropriate asymptotic analysis show that the ratio of the nonaxisymmetric flow to the axisymmetric one is extremely small, thus validating the common neglect of the nonaxisymmetric flow. Therefore a rotating magnetic field may provide beneficial stirring without disturbing the desirable axisymmetric distribution of additives in the liquid. © *1999 American Institute of Physics.* [S1070-6631(99)01407-5]

I. INTRODUCTION

Since most molten semiconductors are good electrical conductors, an externally applied magnetic field can be used to control the motion of the liquid during the growth of single crystals in order to produce better crystals. Recent experiments have shown that certain periodic, transverse magnetic fields, called rotating magnetic fields (RMFs), produce much better solid-solution or alloyed crystals[1,2] and reduce small-scale spatial oscillations of the additive concentration in nearly pure crystals.[3] Most crystal-growth systems have axisymmetric geometries. An RMF is produced by a number of magnet poles which are placed at equally spaced azimuthal positions around the crystal-growth furnace and which are connected to the successive phases of a multiphase electric power source. This arrangement produces an essentially constant magnetic-field pattern which rotates in the azimuthal direction with an angular velocity ω/p, where ω is the circular frequency of the magnetic field and p is the ratio of the number of poles to the number of phases in the power source. The pattern of the RMF depends on p. If $p=1$, e.g., a three-phase power source and three magnet poles, then the RMF is essentially uniform over each $z=$constant plane, where r, θ, z are cylindrical coordinates with the z-axis along the center line of the crystal-growth furnace, with the origin at the middle of the liquid region and with unit vectors $\hat{\mathbf{r}}$, $\hat{\theta}$, $\hat{\mathbf{z}}$. We assume that the magnet poles are axially long enough that the RMF is spatially uniform over the entire liquid region and we restrict our study to $p=1$.

At present, RMFs are being used in Bridgman, floating-zone,[3] and traveling heater method[4] crystal-growth systems. We only consider the Bridgman process where the molten semiconductor is contained in a cylindrical, electrically insulating ampoule and the crystal grows axially from a seed at one end of the ampoule. In order to compute typical values of the important dimensionless parameters, we use the properties of molten silicon with an electrical conductivity $\sigma=10^6$ S/m, density $\rho=2530$ kg/m^3, and dynamic viscosity $\mu=7\times10^{-4}$ Pa-s.[5] The parameter values for gallium-arsenide, indium-phosphide and germanium-silicon do not differ by more than a factor of two from those for silicon. For our typical values, the inside radius of the ampoule $R=1$ cm and $\omega=100\pi$ rad/s (50 Hz).

The periodic applied magnetic field produces electric currents in the electrically conducting liquid, and these currents produce an induced magnetic field which tends to cancel the applied field in the interior of the liquid. The characteristic ratio of the induced to applied magnetic field strengths for an RMF is the shielding parameter, $R_\omega=\mu_p\sigma\omega R^2$, where μ_p is the magnetic permeability of the liquid. Our typical value is $R_\omega=0.0395$, which is definitely small enough to neglect the induced magnetic field,[6,7] so that the applied field penetrates throughout the liquid. There is also an induced field associated with the liquid motion, but it is even smaller.

Three remaining dimensionless numbers complete the set of important parameters. The first is the instantaneous aspect ratio, which is defined as the axial length of the liquid region divided by the inside diameter of the ampoule and which varies from a large value to zero during a crystal-growth process. Since crystal-growth processes are extremely slow, quasisteady solutions for each instantaneous value of the aspect ratio are appropriate. For the other two key parameters, we use the interaction parameter $N=\sigma B^2/\rho\omega$ and the Reynolds number $\mathrm{Re}=\rho\omega R^2/\mu$, both

based on frequency, where B is the magnetic flux density of the spatially uniform RMF. Other pairs of dimensionless parameters, such as Hartmann number and magnetic Taylor number, can be defined as products of powers of N and Re. In a fixed laboratory reference frame, the time scale for inertia is determined by the frequency ω of the periodic forces, so that N and Re are the characteristic ratios of the largest inertial term in the Navier-Stokes equation with the electromagnetic body force term and viscous term, respectively. Our typical values are $N=1.5B^2$ and $\mathrm{Re}=1.14\times10^5$, with B in tesla. If $N\gg1$ and $\mathrm{Re}\gg1$, most of the fluid motion approaches a rigid-body rotation with the RMF,[8,9] while the nonaxisymmetric and axisymmetric flows are both comparable to ωR. However, B ranges from 1 to 10 mT for RMFs currently being used in crystal growth, so that $N\leqslant0.000\,15$ for 50 Hz. For $N\ll1$, the dimensional velocity in the laboratory frame is much smaller than ωR, so that the induced electric field due to the interaction of the melt motion and the RMF is negligible in Ohm's law for the laboratory frame, and the problem governing the leading-order variables becomes two sequential problems.[10] The dimensionless electric current density $\mathbf{j}$, electric potential function ϕ, and electromagnetic (EM) body force due to the interaction of $\mathbf{j}$ and the RMF are determined in the first problem, and then the flow driven by the EM body force is determined in the second problem. The leading-order term for the EM body force in the laboratory frame consists of a steady, axisymmetric, azimuthal force, plus a three-dimensional force whose components vary as the sine or cosine of $2(\theta-\omega t)$ and which we call the nonaxisymmetric body force. If the cylinder is infinitely long and all variables are independent of z, then the nonaxisymmetric body force is irrotational, so that it only produces a nonaxisymmetric pressure and it does not drive any flow.[10] However, for a finite-length cylinder where all or part of the axial electric current is blocked by the ends of the cylinder, the nonaxisymmetric body force is not irrotational and cannot be balanced by a pressure gradient. A consequence of assuming that $N\ll1$ is that, to leading order, the fluid does not respond to the nonaxisymmetric body force because in the laboratory frame this force oscillates with twice the frequency of the RMF, i.e., the velocity produced during a half period of this force is small compared to the velocity produced by the steady, axisymmetric part of the leading-order EM body force.[10,11] Therefore most previous researchers have presented solutions for the steady, axisymmetric flow driven by the azimuthal average of the leading order EM body force due to the RMF.[10]

This paper presents an analytical solution for the unsteady, nonaxisymmetric flow perturbation driven by the nonaxisymmetric body force, i.e., the deviation of the leading-order EM body force from its azimuthal average. The primary purpose of this paper is to quantify the magnitude of the small unsteady nonaxisymmetric flow and hopefully to validate the common neglect of this flow for the RMFs currently used in crystal-growth processes. Our second purpose reflects the current interest in the stability of the steady axisymmetric flow driven by an RMF. Since a small, but finite-amplitude periodic perturbation which is always present may affect the stability of the steady axisymmetric flow, the solutions presented here may be used in future stability analyses.

II. PROBLEM FORMULATION AND SOLUTION

With r and z normalized by R, the boundaries of the fluid region are at $r=1$ and at $z=\pm a$, where $2aR$ is the dimensional length of this region. In the Bridgman crystal-growth process, the aspect ratio a decreases as the crystal grows from one end of the ampoule, but crystal growth is so slow that the motion of the crystal-melt interface can be ignored in the flow problem. The ampoule is an electrical insulator, but the crystal has a nonzero electrical conductivity. For silicon, the electrical conductivity of the crystal $\sigma_s=0.05\sigma$.[5] For $N\gg1$, the parameter which reflects the role of the crystal's electrical conductivity is $\mathrm{Ha}\,\sigma_s/\sigma$, where $\mathrm{Ha}=BR(\sigma/\mu)^{1/2}$ is the Hartmann number. Since the value of Ha is always large when N is large, the crystal is a very important part of the electrical circuit.[9] For $N\ll1$, the parameter reflecting the role of the crystal's conductivity is simply σ_s/σ, or 0.05 for silicon, so that we treat the crystal as an electrical insulator in the present small N asymptotic solution.

We use a noninertial reference frame which rotates with the RMF at the constant angular velocity ω around the z axis. In this rotating frame, the RMF and the flow are both steady, while the ampoule and crystal rotate with an angular velocity $-\omega\hat{\mathbf{z}}$. The dimensional azimuthal liquid velocity in the rotating reference frame equals that in the laboratory frame minus ωRr. Thus the laboratory-frame time derivative in the Navier-Stokes equations becomes $-\omega\partial/\partial\theta$ from the azimuthal convective derivative in the rotating frame. Similarly, the time derivative of the magnetic field in Faraday's law for the laboratory frame becomes an induced electric field $(-\omega rR\hat{\theta})\times B\hat{\mathbf{b}}$ in Ohm's law for the rotating frame. With the $\theta=0$ radius parallel to the spatially uniform RMF, the RMF is $B\hat{\mathbf{b}}$, where the unit vector $\hat{\mathbf{b}}=\cos\theta\hat{\mathbf{r}}-\sin\theta\hat{\theta}$. With the assumption that $R_\omega\ll1$, the dimensionless governing equations in the noninertial rotating reference frame are

$$(\mathbf{v}\cdot\nabla)\mathbf{v}-2\mathbf{v}\times\hat{\mathbf{z}}-r\hat{\mathbf{r}}=-\nabla p+N\mathbf{j}\times\hat{\mathbf{b}}+\mathrm{Re}^{-1}\nabla^2\mathbf{v}, \tag{1a}$$

$$\mathbf{j}=-\nabla\phi+\mathbf{v}\times\hat{\mathbf{b}}, \tag{1b}$$

$$\nabla\cdot\mathbf{v}=0, \tag{1c}$$

$$\nabla\cdot\mathbf{j}=0, \tag{1d}$$

where $\mathbf{v}$ is the liquid's velocity in the rotating frame normalized by ωR, p is the pressure normalized by $\rho\omega^2R^2$, $\mathbf{j}$ is the electric current density normalized by $\sigma\omega RB$, and ϕ is the electric potential function in the rotating frame normalized by ωR^2B. Equation (1a) is the Navier-Stokes equation with the Coriolis acceleration $-2\mathbf{v}\times\hat{\mathbf{z}}$, the centripetal acceleration $-r\hat{\mathbf{r}}$, and the EM body force $N\mathbf{j}\times\hat{\mathbf{b}}$; Eq. (1b) is Ohm's law, Eq. (1c) is conservation of mass, and Eq. (1d) is a solubility condition which insures that a solution for the ignored $O(R_\omega)$ induced magnetic field is possible.

In this rotating reference frame, $\mathbf{v}=-r\hat{\theta}$, plus smaller terms. The O(1) $\mathbf{j}$ and ϕ are governed by Eq. (1d) and Eq. (1b), which becomes

$$\mathbf{j} = -\nabla\phi + r\cos\theta\hat{\mathbf{z}}. \tag{2}$$

The boundary conditions on the electrical variables are

$$j_r = 0 \quad \text{at} \quad r = 1, \tag{3a}$$

$$j_z = 0 \quad \text{at} \quad z = \pm a. \tag{3b}$$

The problem governing $\mathbf{j}$ and ϕ is linear, so that the Fourier components in θ are independent of each other. The only inhomogeneous term in the boundary value problems for the various Fourier components arises from the $r\cos\theta$ term in Eq. (2) through Eqs. (3b), so that only one Fourier component is nonzero and $\phi = \cos\theta\Phi(r,z)$. There is a simple separation-of-variables solution for Φ,[12]

$$\Phi = \sum_{n=1}^{\infty} \frac{2J_1(\lambda_n r)\sinh(\lambda_n z)}{\lambda_n(\lambda_n^2 - 1)J_1(\lambda_n)\cosh(\lambda_n a)}, \tag{4}$$

where J_k is the Bessel function of the first kind and kth order, while λ_n are the roots of $\lambda_n J_0(\lambda_n) - J_1(\lambda_n) = 0$.

We define the axisymmetric velocity $\mathbf{v}_a(r,z)$ as the azimuthal average of $\mathbf{v}$ and the nonaxisymmetric velocity $\mathbf{v}_n(r,\theta,z) = \mathbf{v} - \mathbf{v}_a$. We use the same process to split p into p_a (r,z) and $p_n(r,\theta,z)$. To each order in the asymptotic solution, the equations governing $\mathbf{v}_a$ and p_a are given by the azimuthal averages of Eqs. (1a) and (1b), while the equations governing $\mathbf{v}_n$ and p_n are given by Eqs. (1a) and (1b), each minus its azimuthal average. There are certainly couplings between the two problems beyond the first-order terms. Splitting the problem into axisymmetric and nonaxisymmetric problems before introducing asymptotic expansions reduces the complexity arising from the different possible relationships between the two parameters N and Re.

For the axisymmetric flow, the dimensionless boundary value problem involves a single parameter which is the magnetic Taylor number $T_m = (1/2)\mathrm{Re}^2 N = \rho\omega\sigma B^2 R^4/2\mu^2$. For the axisymmetric problem, inertial or viscous terms dominate if $T_m^{1/2} \gg 1$ or $T_m^{1/2} \ll 1$, respectively. For the nonaxisymmetric problem, inertial or viscous terms dominate if $\mathrm{Re} \gg 1$ or $\mathrm{Re} \ll 1$, respectively. For the steady axisymmetric flow, the viscous boundary layer thickness is reflected by a Reynolds number based on the actual azimuthal velocity, and this Reynolds number is T_m. For the unsteady nonaxisymmetric flow, the direction of the velocity changes twice with each rotation of the magnetic field, so that the boundary layers cannot grow much during the brief period of time while the velocity is in one direction, so that their thickness is reflected by Re based on ω. For practical crystal-growth processes, both T_m and Re are large. The axisymmetric flow is discussed after we present the leading-order solution for the nonaxisymmetric flow.

In the rotating frame, the asymptotic expansions for $\mathbf{v}_a$ and $\mathbf{v}_n$ are

$$\mathbf{v}_a = -r\hat{\theta} + \varepsilon\mathbf{v}_{a0} + \ldots, \tag{5a}$$

$$\mathbf{v}_n = N\mathbf{v}_{n0} + O(\varepsilon N), \tag{5b}$$

where ϵ is a small parameter and the $O(\varepsilon N)$ terms in (5b) arise from the coupling terms, $(\mathbf{v}_{a0}\cdot\nabla)\mathbf{v}_{n0}$ and $(\mathbf{v}_{n0}\cdot\nabla)\mathbf{v}_{a0}$. The value of ϵ depends on T_m and is discussed later. For the nonaxisymmetric flow and for $\mathrm{Re} \geqslant O(1)$, the time derivative in the laboratory frame or the azimuthal convective derivative in the rotating frame is comparable to the $O(N)$ EM body force, so that the leading term in $\mathbf{v}_n$ is $O(N)$. For $\mathbf{v}_{n0}$, we only need $\epsilon \ll 1$, which is also required for (4). Since the pressure balances part of the $O(N)$ nonaxisymmetric EM body force, $p_n = N p_{n0}$, plus smaller terms.

The $O(N)$ terms in Eqs. (1a) and (1b), each minus its azimuthal average, give linear equations governing $\mathbf{v}_{n0}$ and p_{n0},

$$-\frac{\partial v_{rn0}}{\partial\theta} = -\frac{\partial p_{n0}}{\partial r} + \frac{1}{2}\sin(2\theta)\left[r - \frac{\partial\Phi}{\partial z}\right] + \mathrm{Re}^{-1}\left[\nabla^2 v_{rn0} - \frac{v_{rn0}}{r^2} - \frac{2}{r^2}\frac{\partial v_{\theta n0}}{\partial\theta}\right], \tag{6a}$$

$$-\frac{\partial v_{\theta n0}}{\partial\theta} = -\frac{1}{r}\frac{\partial p_{n0}}{\partial\theta} + \frac{1}{2}\cos(2\theta)\left[r - \frac{\partial\Phi}{\partial z}\right] + \mathrm{Re}^{-1}\left[\nabla^2 v_{\theta n0} + \frac{2}{r^2}\frac{\partial v_{rn0}}{\partial\theta} - \frac{v_{\theta n0}}{r^2}\right], \tag{6b}$$

$$-\frac{\partial v_{zn0}}{\partial\theta} = -\frac{\partial p_{n0}}{\partial z} + \frac{1}{2}\sin(2\theta)\left[\frac{\partial\Phi}{\partial r} - \frac{\Phi}{r}\right] + \mathrm{Re}^{-1}\nabla^2 v_{zn0}, \tag{6c}$$

$$\frac{\partial v_{rn0}}{\partial r} + \frac{v_{rn0}}{r} + \frac{1}{r}\frac{\partial v_{\theta n0}}{\partial\theta} + \frac{\partial v_{zn0}}{\partial z} = 0, \tag{6d}$$

where

$$\nabla^2 = \frac{\partial^2}{\partial r^2} + \frac{1}{r}\frac{\partial}{\partial r} + \frac{1}{r^2}\frac{\partial^2}{\partial\theta^2} + \frac{\partial^2}{\partial z^2}. \tag{6e}$$

The azimuthal derivatives on the left sides of Eqs. (6a) through (6c) would be time derivatives in the laboratory frame, reflecting the traditional statement that the nonaxisymmetric velocity is small because the fluid cannot respond during the short half period of the fluctuating EM body force. The EM body force terms involving Φ are known driving terms, since Φ is given by Eq. (4). The boundary conditions are

$$\mathbf{v}_{n0} = 0, \quad \text{at} \quad r = 1, \tag{7a}$$

$$\mathbf{v}_{n0} = 0, \quad \text{at} \quad z = \pm a. \tag{7b}$$

While a numerical solution of Eqs. (6) and (7) for any value of Re would be quite simple, our typical value of Re is 1.14×10^5, so that an asymptotic solution for $\mathrm{Re} \gg 1$ is certainly appropriate. For $\mathrm{Re} \gg 1$, the liquid region is divided into a core region and boundary layers with $O(\mathrm{Re}^{-1/2})$ thickness adjacent to each boundary. In the core, the Fourier series in θ for each variable has only one nonzero component, which is associated with the known driving functions in Eqs. (6a)–(6c), so that

$$v_{rn0} = \cos(2\theta)V_r(r,z), \tag{8a}$$

$$v_{\theta n0} = \sin(2\theta)V_\theta(r,z), \tag{8b}$$

$$v_{zn0} = \cos(2\theta)V_z(r,z), \tag{8c}$$

$$p_{n0}=\sin(2\theta)P(r,z). \tag{8d}$$

Neglecting $O(\mathrm{Re}^{-1})$ terms in the core, Eqs. (6) give

$$V_r=-\frac{1}{2}\frac{\partial P}{\partial r}+\frac{1}{4}\left[r-\frac{\partial \Phi}{\partial z}\right], \tag{9a}$$

$$V_\theta=\frac{P}{r}-\frac{1}{4}\left[r-\frac{\partial \Phi}{\partial z}\right], \tag{9b}$$

$$V_z=-\frac{1}{2}\frac{\partial P}{\partial z}+\frac{1}{4}\left[\frac{\partial \Phi}{\partial r}-\frac{\Phi}{r}\right], \tag{9c}$$

$$\frac{\partial^2 P}{\partial r^2}+\frac{1}{r}\frac{\partial P}{\partial r}-\frac{4P}{r^2}+\frac{\partial^2 P}{\partial z^2}=0. \tag{9d}$$

Inside the boundary layer adjacent to $r=1$, $v_{rn0}=O(\mathrm{Re}^{-1/2})$, and inside the boundary layers adjacent to the ends at $z=\pm a$, $v_{zn0}=O(\mathrm{Re}^{-1/2})$. Therefore, the boundary conditions on the core solution neglecting $O(\mathrm{Re}^{-1/2})$ terms are

$$V_r=0, \quad \text{at } r=1, \tag{10a}$$

$$V_z=0, \quad \text{at } z=\pm a. \tag{10b}$$

The separation-of-variables solution for the core is

$$P=\frac{r^2}{4}+\sum_{k=1}^{\infty} B_k J_2(\alpha_k r)\frac{\cosh(\alpha_k z)}{\sinh(\alpha_k a)} - \sum_{n=1}^{\infty}\frac{\lambda_n J_2(\lambda_n r)\cosh(\lambda_n z)}{(\lambda_n^2-1)(\lambda_n^2-2)J_1(\lambda_n)\cosh(\lambda_n a)}, \tag{11a}$$

where

$$B_k=\frac{4\alpha_k}{(\alpha_k^2-4)J_2(\alpha_k)}\sum_{n=1}^{\infty}\frac{\tanh(\lambda_n a)}{(\alpha_k^2-\lambda_n^2)\lambda_n(\lambda_n^2-1)}, \tag{11b}$$

and α_k are the roots of $\alpha_k J_1(\alpha_k)-2J_2(\alpha_k)=0$.

For the boundary layer adjacent to $r=1$, we introduce the stretched coordinate $\xi=\mathrm{Re}^{1/2}(r-1)$. Neglecting $O(\mathrm{Re}^{-1/2})$ terms, the solution which satisfies the boundary-layer equations and Eqs. (7a) and which matches the core solution is

$$v_{rn0}=0, \tag{12a}$$

$$p_{n0}=\sin(2\theta)P(1,z), \tag{12b}$$

$$v_{\theta n0}=V_\theta(1,z)\{\cos(2\theta)\exp(\xi)\sin(\xi) + \sin(2\theta)[1-\exp(\xi)\cos(\xi)]\}, \tag{12c}$$

$$v_{zn0}=V_z(1,z)\{\cos(2\theta)[1-\exp(\xi)\cos(\xi)] - \sin(2\theta)\exp(\xi)\sin(\xi)\}. \tag{12d}$$

For the boundary layer adjacent to $z=a$, we introduce the stretched coordinate $\zeta=\mathrm{Re}^{1/2}(z-a)$. Neglecting $O(\mathrm{Re}^{-1/2})$ terms, the solution which satisfies the boundary-layer equations and Eq. (7b), and which matches the core solution, is

$$v_{zn0}=0, \tag{13a}$$

$$p_{n0}=\sin(2\theta)P(r,a), \tag{13b}$$

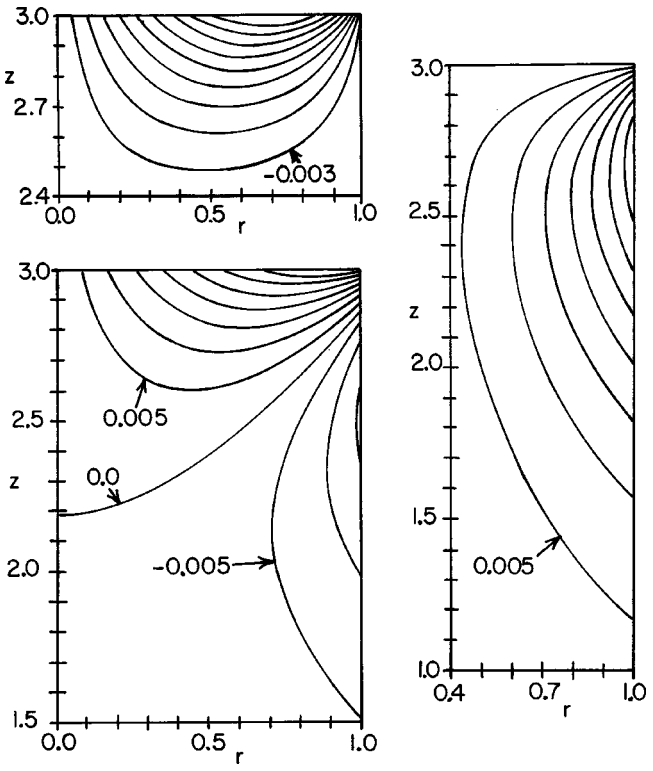

FIG. 1. Contours of V_r, V_θ and V_z for the core solution. (a) $V_r=-0.003n$ for $n=1$ to 9. (b) $V_\theta=0.005n$ for $n=-3$ to 7. (c) $V_z=0.005n$ for $n=1$ to 7.

$$v_{rn0}=V_r(r,a)\{\cos(2\theta)[1-\exp(\zeta)\cos(\zeta)] - \sin(2\theta)\exp(\zeta)\sin(\zeta)\}, \tag{13c}$$

$$v_{\theta n0}=V_\theta(r,a)\{\cos(2\theta)\exp(\zeta)\sin(\zeta) + \sin(2\theta)[1-\exp(\zeta)\cos(\zeta)]\}. \tag{13d}$$

The boundary layer at $z=-a$ is the mirror image of the one at $z=a$. Thus each boundary layer matches the O(1) tangential velocities in the core and satisfies the no-slip conditions at the boundary with a structure which is identical to that for the boundary layer on an oscillating flat plate.

III. RESULTS

Contour plots of the core variables V_r, V_θ, and V_z for $a=3$ are presented in Fig. 1. Since V_r and V_θ are even functions of z, while V_z is an odd function, results are only presented for $0\leqslant z\leqslant a$. For $a=3$, all velocities are essentially zero for $0\leqslant z\leqslant 1$. The rotational part of the nonaxisymmetric EM body force arises from the blockage of the axial electric currents by the insulating ends at $z=\pm a$. The results show that the nonaxisymmetric flow is confined to an axial length equal to two ampoule radii near each end. Therefore the results are independent of a for $a\geqslant 2$.

Equations (8) and the results in Fig. 1 indicate that the nonaxisymmetric flow involves four circulations. Since these circulations are symmetric about the four planes at $\theta=0$, $\theta=\pi$, and $\theta=\pm\pi/2$, which separate the four circulations, we only describe the circulation for $0\leqslant\theta\leqslant\pi/2$. Two closed toroidal-like surfaces are presented in Fig. 2, where the center line of each torus is a closed streamline for the nonaxi-

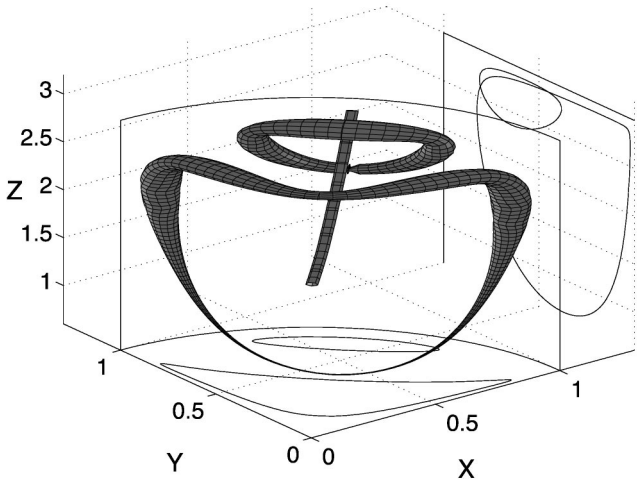

FIG. 2. Two closed toroidal surfaces whose center lines are closed streamlines and whose radius is proportional to the magnitude of the velocity. The two streamlines pass through the $\theta=\pi/4$ plane at $r=0.2$, $z=2.9$ and $r=0.8$, $z=2.9$. The projections of the streamlines on a horizontal plane and a vertical plane are also shown. The velocity is zero along the line in the $\theta=\pi/4$ plane.

symmetric flow and the radius of the torus at each point along the streamline is proportional to the magnitude of the local nonaxisymmetric flow velocity. The other curve in Fig. 2 is the line in the $\theta=\pi/4$ plane where $V_\theta=0$. Since V_r and V_z are zero in this plane, the velocity is zero at this line, so the nonaxisymmetric flow circulates around this line. The values of V_θ in Fig. 1(b) represent the velocity across the plane at $\theta=\pi/4$, with flow in the $+\theta$ direction for the $V_\theta>0$ near $z=a$ and with flow in the $-\theta$ direction for the $V_\theta<0$ near $r=1$. The flow in the $-\theta$ direction across the $\theta=\pi/4$ plane near $r=1$ first turns and flows axially toward $z=a$ near $r=1$, as reflected by $V_z>0$ in Fig. 1(c). The flow then turns and flows radially inward near $z=a$, as reflected by $V_r<0$ in Fig. 1(a). The flow then turns to flow in the $+\theta$ direction back across the $\theta=\pi/4$ plane, as reflected by $V_\theta>0$ near $z=a$ in Fig. 1(b). Once beyond the $\theta=\pi/4$ plane, the flow first flows radially outward near $z=a$, again reflected by $V_r<0$ in Fig. 1(a), and then flows axially toward the plane of symmetry at $z=0$ near $r=1$, again reflected by $V_z>0$ in Fig. 1(c). Finally the flow turns to cross the $\theta=\pi/4$ plane in the $-\theta$ direction, thus completing the circulation. The minimum value of V_r in Fig. 1(a) is -0.0308, V_θ in Fig. 1(b) ranges from -0.0163 to 0.0413, and the maximum value of V_z in Fig. 1(c) is 0.0391.

IV. COMPARISON OF AXISYMMETRIC AND NONAXISYMMETRIC FLOWS

For the axisymmetric flow, we introduce $\hat{\mathbf{v}}_a=N^{-1/2}(\mathbf{v}_a+r\hat{\theta})$, so that $\hat{\mathbf{v}}_a$ is the steady axisymmetric velocity in the laboratory frame, normalized by $N^{1/2}\omega R$. Then the leading term in the asymptotic expansion of $\hat{\mathbf{v}}_a$ for $N\ll 1$ depends only on the magnetic Taylor number $Tm=(1/2)\mathrm{Re}^2N$, whose value is 9.7×10^5 for our typical Bridgman crystal-growth process with $B=10$ mT and 50 Hz. For electromagnetic stirring during the continuous casting of steel or aluminum, Davidson[12] presented asymptotic solutions for $\hat{\mathbf{v}}_a$ with $Tm\gg1$. Two differences between crystal growth and continuous casting are (1) that the liquid-solid interface is concave for casting so that no part of this interface is parallel to the axis of rotation, and (2) that the electrical conductivity of the solid is comparable to that of the liquid so that the solid does not block the axial electric currents, and the nonaxisymmetric part of the EM body force remains irrotational and does not drive an unsteady nonaxisymmetric flow. Davidson's solution applies to our axisymmetric flow away from the ampoule wall at $r=1$, which is parallel to the axis of rotation. In Davidson's solution, there is an inviscid core and Ekman layers with an $O(Tm^{-1/3})$ thickness adjacent to the solid surfaces at $z=\pm a$. In both the core and Ekman layers, $\hat{v}_{a\theta}$ is $O(Tm^{1/6})$; in the Ekman layer, $\hat{v}_{ar}$ and $\hat{v}_{az}$ are $O(Tm^{1/6})$ and $O(Tm^{-1/6})$, respectively; and in the core, $\hat{v}_{ar}$ and $\hat{v}_{az}$ are both $O(Tm^{-1/6})$. The secondary flow in each $\theta=$constant plane consists of a strong radially inward jet inside each Ekman layer which turns to enter the core at $z=\pm a$. In the core, this flow turns to become radially outward. For our crystal-growth application, we also have a Stewartson layer with an $O(Tm^{-1/6})$ thickness adjacent to the ampoule wall at $r=1$ and corner regions with $O(Tm^{-1/6})\times O(Tm^{-1/6})$ dimensions at $r=1$ and $z=\pm a$. The Stewartson layer (1) matches the $\hat{v}_{a\theta}$ in the core, which increases monotonically with r, and satisfies the no-slip condition on $\hat{v}_{a\theta}$ at $r=1$, and (2) accepts the radially outward flow from the core and delivers it to the corner regions, which return it to the Ekman layers at $r=1$. While $\hat{v}_{a\theta}$ is also $O(Tm^{1/6})$ inside the Stewartson layer and corner regions, the secondary flow inside these regions is larger than that in the core and Ekman layers, namely $O(Tm^{-1/12})$ rather than $O(Tm^{-1/6})$. This slightly stronger secondary flow, which is confined to the Stewartson layer and corner regions, arises because there is an axial variation of the $O(Tm^{1/6})$ $\hat{v}_{a\theta}$ inside the Stewartson layer, while the axial variation of $\hat{v}_{a\theta}$ in the core is $O(Tm^{-1/2})$.

The asymptotic solution for the axisymmetric flow with $Tm\gg1$ provides some very valuable insights, but it cannot provide accurate predictions because it assumes that $Tm^{-1/12}\ll1$, while $Tm^{-1/12}$ is not small for practical processes. For our example, $Tm^{-1/12}=0.32$. The steady axisymmetric flow may involve either a Taylor-Couette instability inside the Stewartson layer or a shear-layer instability inside the Ekman layers. The shear layer instability has not yet been investigated but models of the Taylor-Couette instability indicate that the critical value of Tm lies between 10^5 and 10^6, for various values of a.[13,14] Thus the solution for $Tm\gg1$ does not provide accurate predictions for any stable axisymmetric flow. The most accurate results are provided by numerical solutions with adequate resolution of the Ekman and Stewartson layers.

In terms of our asymptotic expansions (5), we take $\varepsilon=N^{1/2}$ and consider $\mathbf{v}_{a0}$ to depend on Tm, which has a large value. For $a=1$ and $Tm=10^5$, numerical solutions for the steady axisymmetric flow indicate that the maximum values of v_{a0r}, $v_{a0\theta}$, and v_{a0z} are 0.3, 2.5, and 0.14, respectively.

These values are $O(Tm^{1/6})$, $O(Tm^{1/6})$, and $O(Tm^{1/12})$, respectively, the latter associated with the $O(Tm^{-1/12})$ secondary flow inside the Stewartson layer. We can now compare these values times $N^{1/2}$ to the maximum magnitudes of $v_{n0r}=0.031$, $v_{n0\theta}=0.041$, and $v_{n0z}=0.039$ in Fig. 1, times N. The maximum ratio of a nonaxisymmetric velocity to its axisymmetric counterpart is roughly $0.3N^{1/2}$ for the axial velocity. The maximum axial axisymmetric and nonaxisymmetric velocities occur at roughly the same position. Therefore we conclude that the nonaxisymmetric velocity is indeed negligible for practical crystal-growth applications of rotating magnetic fields.

ACKNOWLEDGMENTS

This research was supported by the U.S. National Aeronautics and Space Administration under Grant No. NAG 8-1453 and by the U.S. National Science Foundation under Grant No. CTS 94-19484.

[1]M. Salk, M. Fiederle, K. W. Benz, A. S. Senchenkov, A. V. Egorov, and D. G. Matioukhin, ''CdTe and $CdTe_{0.9}Se_{0.1}$ crystals grown by the travelling heater method under a rotating magnetic field,'' J. Cryst. Growth **138**, 161 (1994).

[2]M. Fiederle, C. Eiche, W. Joerger, M. Salk, A. S. Senchenkov, A. V. Egorov, D. G. Ebling, and K. W. Benz, ''Radiation detector properties of $CdTe_{0.9}Se_{0.1}$:Cl crystals grown under microgravity in a rotating magnetic field,'' J. Cryst. Growth **166**, 256 (1996).

[3]P. Dold, A. Croll, K. W. Benz, and F. Szofran, ''Halbleiterkristallzuchtung im magnetfeld und unter mikrogravitation,'' DARA Workshop, Berlin, 23-24 January 1997.

[4]C. K. Ghaddar, C. K. Lee, S. Motakef, and D. C. Gillies, ''Numerical simulation of THM growth of CdTe in presence of rotating magnetic field,'' (submitted).

[5]P. Sabhapathy and M. E. Salcudean, ''Numerical study of Czochralski growth of silicon in an axisymmetric magnetic field,'' J. Cryst. Growth **113**, 164 (1991).

[6]L. Martin Witkowski and P. Marty, ''Effect of a rotating magnetic field of arbitrary frequency on a liquid metal column,'' Eur. J. Mech. B/Fluids **17**, 239 (1998).

[7]K. Mazuruk, N. Ramachandran, M. P. Volz, and D. Gillies, ''Study of frequency effects of a rotating magnetic field on fluid flow in vertical cylinders,'' Soc. Photo-Opt. Instrum. Eng. **3123**, 262 (1997).

[8]A. Alemany and R. Moreau, ''Ecoulement d'un fluide conducteur de l'electricite en presence d'un champ magnetique tournant,'' J. Mec. **16**, 625 (1977).

[9]J. S. Walker, ''Bridgman crystal growth with a strong, low-frequency, rotating magnetic field,'' J. Cryst. Growth **192**, 318 (1998).

[10]P. A. Davidson and J. C. R. Hunt, ''Swirling recirculating flow in a liquid-metal column generated by a rotating magnetic field,'' J. Fluid Mech. **185**, 67 (1987).

[11]Y. M. Gelfgat, L. A. Gorbunov, and V. Kolevzon, ''Liquid metal flow in a finite-length cylinder with a rotating magnetic field,'' Exp. Fluids **15**, 411 (1993).

[12]P. A. Davidson, ''Swirling flow in an axisymmetric cavity of arbitrary profile, driven by a rotating magnetic field,'' J. Fluid Mech. **245**, 669 (1992).

[13]P. Marty, L. Martin Witkowski, P. Trombetta, T. Tomasino, and J. P. Garandet, ''On the stability of rotating MHD flows,'' *Transfer Phenomena in Magnetohydrodynamic and Electroconducting Flows*, edited by A. Alemany, P. Marty, and J. P. Thibault (Kluwer, Dordrecht, 1999).

[14]T. Kaiser and K. W. Benz, ''Taylor vortex instabilities induced by a rotating magnetic field: A numerical approach,'' Phys. Fluids **10**, 1104 (1998).